NASA Technical Memorandum 102527

# Thermal Radiation Characteristics of Nonisothermal Cylindrical Enclosures Using a Numerical Ray Tracing Technique

Joseph F. Baumeister
*Lewis Research Center*
*Cleveland, Ohio*

Prepared for the
5th Thermophysics and Heat Transfer Conference
cosponsored by the AIAA and ASME
Seattle, Washington, June 18–20, 1990

NASA

# THERMAL RADIATION CHARACTERISTICS OF NONISOTHERMAL CYLINDRICAL ENCLOSURES USING A NUMERICAL RAY TRACING TECHNIQUE

Joseph F. Baumeister
National Aeronautics and Space Administration
Lewis Research Center
Cleveland, Ohio 44135

E-5335

## ABSTRACT

Analysis of energy emitted from simple or complex cavity designs can lead to intricate solutions due to nonuniform radiosity and irradiation within a cavity. A numerical ray tracing technique was applied to simulate radiation propagating within and from various cavity designs. To obtain the energy balance relationships between isothermal and nonisothermal cavity surfaces and space, the computer code NEVADA was utilized for its statistical technique applied to numerical ray tracing. The analysis method was validated by comparing results with known theoretical and limiting solutions, and the electrical resistance network method. In general, for nonisothermal cavities the performance (apparent emissivity) is a function of cylinder length-to-diameter ratio, surface emissivity, and cylinder surface temperatures. The extent of nonisothermal conditions in a cylindrical cavity significantly affects the overall cavity performance. Results are presented over a wide range of parametric variables for use as a possible design reference.

## NOMENCLATURE

| | |
|---|---|
| $A$ | surface area |
| $A_{out}$ | projected surface area at cavity exit |
| $B$ | radiation interchange factor |
| $E_{out}$ | energy emitted per unit time from the cavity |
| $F$ | geometric configuration factor or blackbody view factor |
| $T$ | absolute temperature |
| $\varepsilon$ | surface emissivity value |
| $\varepsilon_a$ | apparent emissivity |
| $\sigma$ | Stefan-Boltzmann constant |

Subscripts:

| | |
|---|---|
| C | cylinder |
| D | disk |
| i,j | $i^{th}$ and $j^{th}$ surfaces |
| n | total number or nth cavity surfaces |
| $\infty$ | space (projected out cavity), infinity |

## INTRODUCTION

The thermal radiation characteristics of partially enclosed surfaces (cavities or enclosures) are of great interest and have resulted in considerable amounts of work in this area. The basic principles of radiation exchange for cavity surfaces lead to complex enclosure theories. Each cavity surface may emit multiple reflecting radiation which can be partially or totally absorbed within the cavity or emitted to its surroundings. Depending on the cavity surface properties and geometry, the energy leaving the cavity may be composed of direct surface emission plus possible reflected energy. The term radiosity refers to the rate of total radiation (combined emission and reflected) leaving a surface and the term irradiation refers to the rate of total radiation incident on a surface. The nonuniform radiation distribution on cavity surfaces results in complex integral equation formulations. Various theoretical techniques have been applied to isothermal and nonisothermal cavities which generally require integration of multiple equations and numerical iteration techniques. The analysis would be further complicated by introducing multiple surface properties and various temperature profiles within complex cavity configurations. The process of analyzing simple or complex cavity geometries may be simplified by applying a numerical ray tracing approach to simulate the nonuniform radiation propagation.

Various types of cavity problems exist. Sparrow (1963, 1966) has presented theoretical solutions for various isothermal gray-diffuse cylindrical geometries with uniform emissivity throughout the cavity. Due to the complicated theoretical solutions required for non-isothermal cavities with various internal surface emissivity values, a ray tracing procedure was applied to solve for the energy emitted from the cavities and is the subject of this paper. A schematic diagram of the analyzed cylindrical cavity is shown in Figs. 1 and 2. Figure 1 displays the uniform cylinder wall temperature case whereas Fig. 2 displays the linearly varying cylinder wall temperature with wall distance case. A numerical ray tracing code that simulates the electromagnetic theory of radiation will be used for analyzing these cavities. The numerical approach solves for the total energy out of the cavity from its individual contributing gray-diffuse cavity sections.

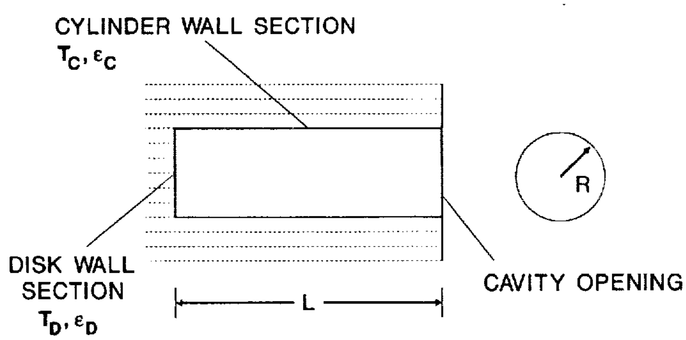


FIGURE 1. - CIRCULAR CYLINDRICAL CAVITY, CROSS SECTION.

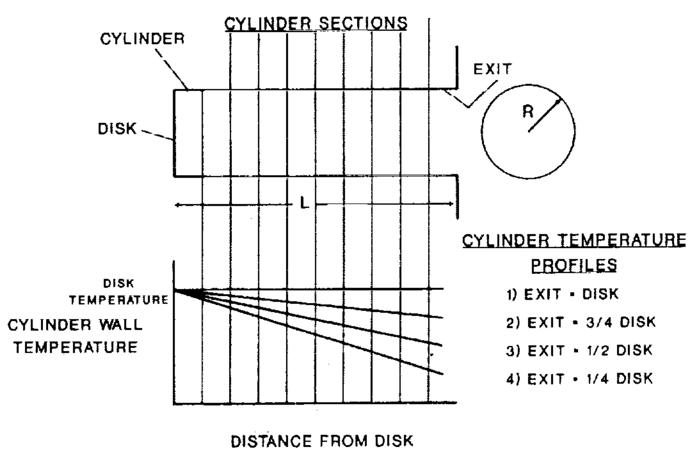


FIGURE 2. - CIRCULAR CYLINDRICAL CAVITY DISPLAYING THE LINEAR WALL TEMPERATURE PROFILES.

There were two basic goals associated with this cavity radiation analysis. The first goal was to validate the numerical ray tracing approach for use in studying complex cavities of various geometries, and the second was to determine the effects of parametric variations on cavity performance. The parametric studies would examine the relationships between a range of cavity dimensions, surface properties, and temperature distributions which may provide insight into radiation propagation for nonisothermal cylindrical cavities and prove useful for design applications. The isothermal analysis of Fig. 1 will be compared to a known theoretical solution, limiting solutions, and a resistance network method as a validation check.

## METHOD OF ANALYSIS

There are several varieties of thermal analysis codes available to model energy flux distributions for various geometries. Each code may have different solution techniques and advantages. The Net Energy Verification And Determination Analyzer (NEVADA) program (Turner, 1988), was selected to simulate the radiation propagation within a cylindrical cavity. NEVADA is a software package consisting of several programs in which a Monte-Carlo mathematical technique is applied to radiation propagation. The NEVADA program was attractive to use because of its ability to handle diffuse or specular radiation and, most importantly, complex geometries.

In the NEVADA code, a statistical numerical method using the Monte-Carlo technique is applied to a ray tracing procedure to model radiation exchange. The ray tracing procedure mathematically traces emitted rays (simulating emitted radiation) as they propagate throughout the cavity. Each ray leaving a surface is considered a bundle of photons. Each photon bundle carries equal, discrete, amounts of energy. The path of the bundles (rays) may interact with various surfaces, all of which may reduce the energy of the bundle. The interacting surfaces may have different thermal properties and geometric configurations that may affect each bundle's propagation differently. By accounting for all the emitted bundles as they propagate throughout the cavity, percentages of incident and absorbed energy at desired locations can be computed. The percentages of absorbed energies are then applied to energy balance equations.

## ANALYSIS

In studying cylindrical cavity type configurations, the overall performance of a cavity is defined as an apparent emissivity. The apparent emissivity is the actual amount of energy leaving the cavity compared with that radiated by a blackbody at disk temperature and projected exit area, or:

$$\varepsilon_a = \frac{E_{out}}{\sigma A_{out}\left(T_D^4 - T_\infty^4\right)} \qquad (1)$$

This apparent emissivity relates direct emitted and reflected radiation leaving the cavity to blackbody radiation. Due to the nonuniform distribution of radiation within the cavity (radiosity and irradiation), calculating the energy emitted from the cavity becomes complicated. Approximate analytical solutions for the radiation exchange integral equations were first derived by Buckley (1927, 1928) and Eckert (1935) and numerically integrated to greater accuracy by Sparrow and Albers (1960).

The numerical ray tracing technique enables one to evaluate the radiation heat transfer from a multi-sectioned cavity to its various sections and the radiation projected out the cavity. The numerical ray tracing technique actually maps radiation as it propagates from surface to surface, and can be applied to the heat transfer equation as:

$$E_{i \to j} = \varepsilon_i \sigma A_i B_{i \to j}\left(T_i^4 - T_j^4\right) \qquad (2)$$

The $i$ and $j$ represent various sections of cavity surfaces such as its circular base $D$, the cylindrical walls $C$, or its opening (space). The blackbody view factor $F$ is replaced by the radiation interchange factor $B$ (obtained from the numerical ray tracing technique) which represents real surface radiation exchange. The radiation interchange factor is a function of the blackbody view factor and the emissivity from all energy exchanging surfaces. The radiation interchange factor is the fraction of emitted energy by a real surface $i$, that is absorbed by a real surface $j$, including all reflections from other real surfaces including surface $i$. For this cavity analysis the surfaces are emitting and reflecting diffuse radiation. The apparent emissivity for a multisection cavity where $n$ represents the total number of individual surface sections becomes:

$$\varepsilon_a = \frac{\sum_{i=1}^{n} \varepsilon_i \sigma A_i B_{i\to\infty}\left(T_i^4 - T_\infty^4\right)}{\sigma A_{out}\left(T_D^4 - T_\infty^4\right)} \tag{3}$$

By use of the numerical ray tracing approach a cavity can be divided into any number of desirable sections within computer computational limits. The isothermal and nonisothermal uniform cavity wall temperature analysis divides the cavity into two sections. The circular base $D$ and cylindrical walls $C$ comprise the cavity model as shown in Fig. 1. For the geometry in Fig. 1, Eq. (3) reduces to:

$$\varepsilon_a = \frac{\varepsilon_D \sigma A_D B_{D\to\infty}\left(T_D^4 - T_\infty^4\right) + \varepsilon_C \sigma A_C B_{C\to\infty}\left(T_C^4 - T_\infty^4\right)}{\sigma A_{out}\left(T_D^4 - T_\infty^4\right)} \tag{4}$$

For the linear cavity wall temperature analysis the wall is divided into ten cylindrical sections as shown in Fig. 2.

There are two limiting cases which are used in validating the numerical results applied in Eq. (4) for the uniform cavity wall temperature analysis. The first limiting case applies when the $L/R$ value approaches zero. In this case:

$$A_C \to 0 \tag{5}$$

$$\text{then } B_{D\to\infty} = F_{D\to\infty} = 1 \tag{6}$$

and Eq. (4) simplifies to:

$$\varepsilon_a\Big|_{L/R\to 0} = \varepsilon_D \tag{7}$$

So for extremely small cylinder cavities where $L/R$ approaches zero, the limiting solution for the apparent emissivity becomes the disk surface emissivity value.

The second limiting solution concerns the case where the uniform cylindrical wall temperature and the environmental temperature approach absolute zero, and the surface emissivity value of the cylindrical wall approaches 1 (complete absorption without emission). Thus, if:

$$T_C \to 0 \quad \text{and} \quad T_\infty \to 0 \tag{8}$$

Eq. (4) reduces to:

$$\varepsilon_a\Big|_{T_C = 0} = \varepsilon_D B_{D\to\infty} \tag{9}$$

For a limiting solution where $\varepsilon_D = \varepsilon_C \to 1$, the cavity walls simulate a blackbody absorbing all incident radiation making $B_{D\to\infty} = F_{D\to\infty}$:

$$\varepsilon_a\Big|_{\substack{T_C = 0 \\ \varepsilon_C = 1}} = F_{D\to\infty} \tag{10}$$

Thus, for this limiting solution the apparent emissivity becomes the disk surface view factor out the cavity opening. The uniform cavity wall temperature analysis included evaluating the cylindrical walls with an emissivity of 0.9 case to simulate near blackbody effects for a limiting case comparison. In addition, various uniform cavity wall temperature cases were also solved using the standard resistance network method (Holman, 1986), which models only uniform radiosity and irradiation, as shown in Fig. 3.

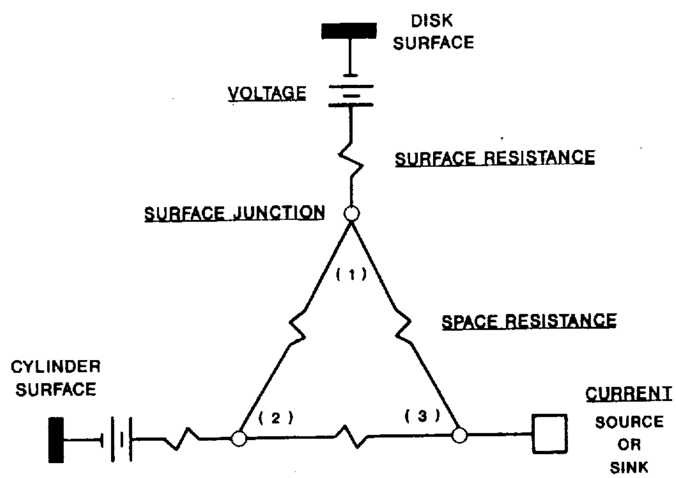


**FIGURE 3. - CAVITY RADIATION NETWORK.**

## DISCUSSION OF RESULTS

The apparent emissivity results for the isothermal cavities are plotted in Fig. 4 for various $L/R$ values and a range of surface emissivity values for diffusely reflecting cavity components. For isothermal cavities with large surface emissivity values and cylinder lengths significantly larger than the cavity radius, the results simulate an infinitely deep cavity as shown in Fig. 4. As a validation check of the analytical method, Fig. 4 displays the apparent emissivity distribution for an isothermal numerical ray tracing analysis against Sparrow's theoretical approach and the limiting solution of Eq. (7). The numerical ray tracing results compared exactly with Sparrow's points and agree with the limiting solution for this isothermal case.

The resistance network method was also applied in analyzing emitted energy from isothermal cylindrical cavity configurations as a possible validation check and to evaluate limiting solution criteria for use as a possible simplified solution technique. Table 1 displays apparent emissivity results from the numerical

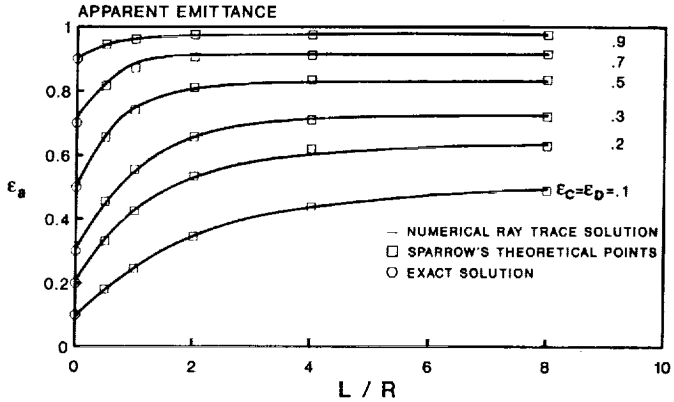


FIGURE 4. - APPARENT EMITTANCE RESULTS FOR DIFFUSELY REFLECTING ISOTHERMAL CYLINDRICAL CAVITIES.

TABLE 1, APPARENT EMISSIVITY RESULTS
RAY TRACING AND RESISTANCE NETWORK METHOD
(ISOTHERMAL CYLINDRICAL CAVITY)

| | APPARENT EMISSIVITY RESULTS | | | | | | | |
|---|---|---|---|---|---|---|---|---|
| | L/R = 0.5 | | L/R = 1.0 | | L/R = 2.0 | | L/R = 4.0 | |
| CAVITY EMISSIVITY | RAY TRACING | R.N.M. | RAY TRACING | R.N.M. | RAY TRACING | R.N.M. | RAY TRACING | R.N.M. |
| .1 | .180 | .181 | .248 | .250 | .347 | .367 | .448 | .499 |
| .2 | .329 | .332 | .425 | .428 | .535 | .555 | .607 | .691 |
| .3 | .455 | .459 | .557 | .562 | .656 | .682 | .711 | .791 |
| .5 | .657 | .662 | .743 | .749 | .811 | .833 | .830 | .899 |
| .7 | .814 | .819 | .876 | .874 | .909 | .921 | .915 | .952 |
| .9 | .946 | .945 | .964 | .964 | .977 | .978 | .980 | .972 |

RAY TRACING = NUMERICAL RAY TRACING TECHNIQUE
R.N.M. = RESISTANCE NETWORK METHOD

ray tracing technique and the resistance network method for several cavity dimensions. For relatively small cavities (L/R less than 2), for practical purposes, the resistance network analysis resulted in exact agreement with the cavity technique applied with Eq. (3) and Sparrow's solution. In these shallow cavities the resistance network method accurately predicts the energy out the cavity for the entire range of surface emissivity values. For cavities with L/R dimensions larger than 2, the difference between the two analysis methods becomes evident. The L/R = 4 results display a widening discrepancy between results at lower cavity emissivity values. This results from the resistance network method requiring assumptions for equal energy distributions on individual surface sections (radiosity and irradiation). To satisfy the requirements the cavity can be sectioned so the energy distribution is approximately uniform over each surface. Once proper cavity sectioning is achieved, the results, for practical purposes, agree exactly with the numerical ray tracing technique and Sparrow's theoretical results. Therefore, for cavities with L/R dimensions greater than 2, the resistance network method requires sectioning the cylindrical walls into smaller individual surfaces. The problem associated with the use of the resistance network method is properly sectioning the cavity to achieve uniform energy distribution within each surface, which may also result in complicated view factor relationships and a large set of simultaneous equations to solve.

Comparing results derived from the various techniques applied to multisectioned isothermal cylindrical cavities reveals that using Eq. (3) with the numerical ray tracing technique can properly evaluate the total energy emitted from the cavities, and the energy emitted from individual cavity sections. With this validation of the ray tracing technique, it can now be applied with greater confidence in analyzing more complicated cavity designs. This type of technique also applies to the energy exchanged between individual sections within the cavity.

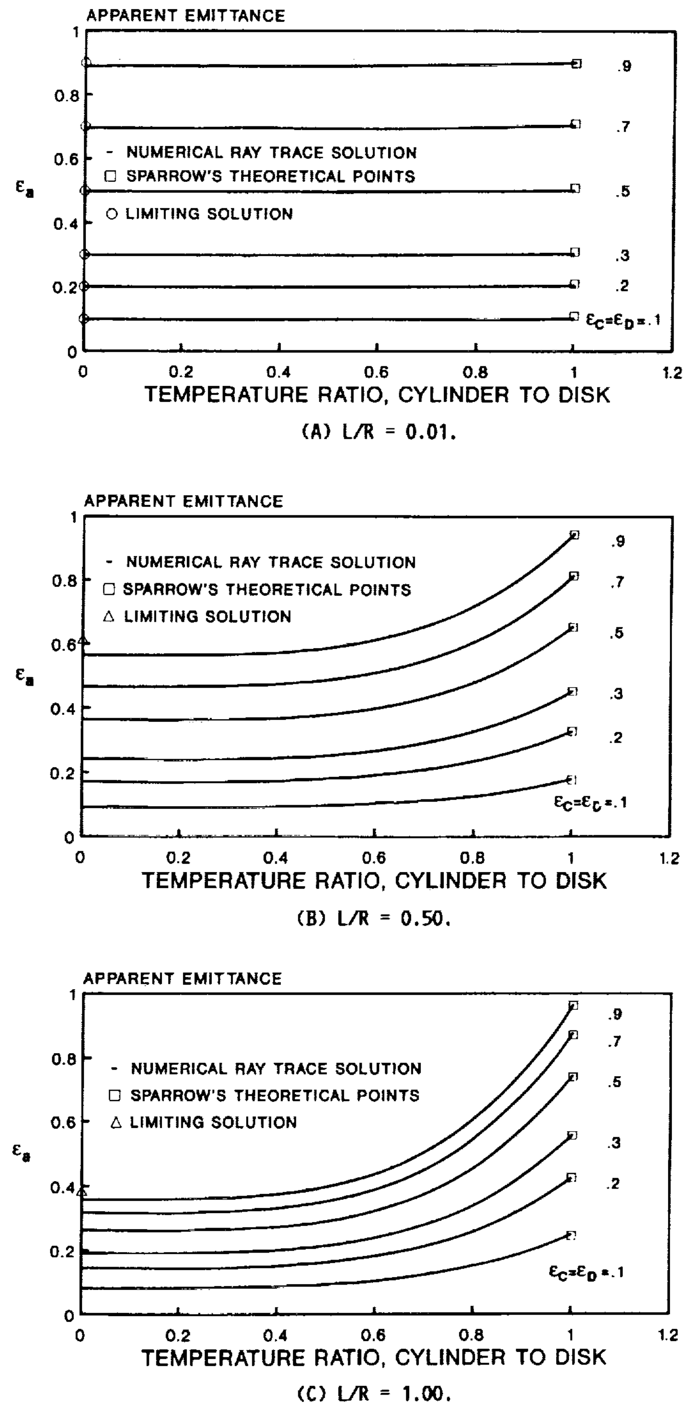


FIGURE 5. - APPARENT EMITTANCE AS A FUNCTION OF TEMPERATURE.

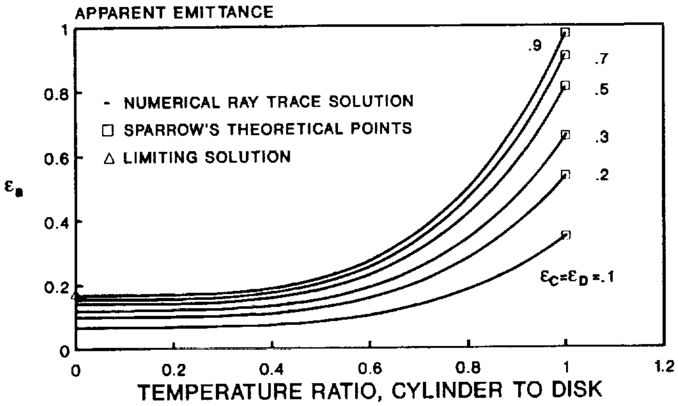


(D) L/R = 2.00.

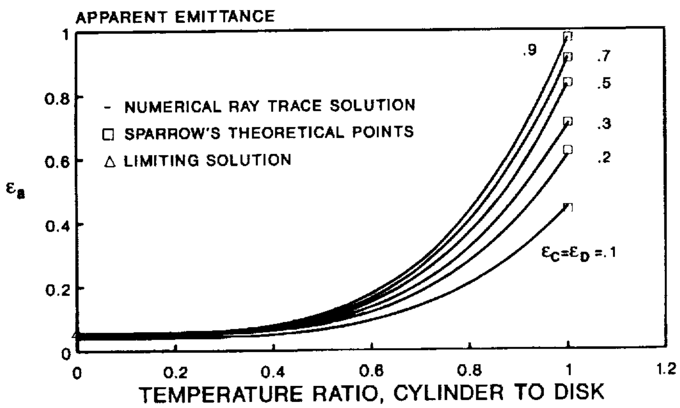


(E) L/R = 4.00.

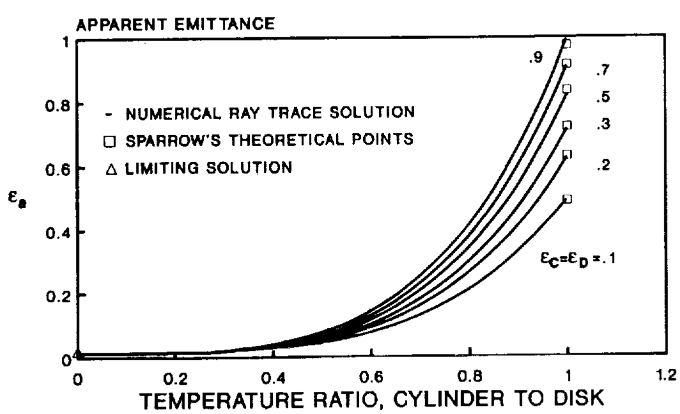


(F) L/R = 8.00.

FIGURE 5. - CONCLUDED.

For nonisothermal cavities with uniform cylinder wall temperatures, Figs. 5(a) to (f) were developed to display the temperature relationships between the disk and cylinder wall surfaces, surface emissivity values, and L/R effects on the apparent emissivity based on Eq. (4). The temperature ratio on the x-axis, cylinder to disk, represents the following equation for environmental temperatures at absolute zero:

$$\text{Temperature ratio} = \frac{T_C - T_\infty}{T_D - T_\infty} = \frac{T_C}{T_D} \qquad (11)$$

Inspection of the curves reveals that regions exist where the apparent emissivity results are dominated by cavity cylinder temperatures and surface emissivity values, except for considerably smaller cavities. For each analyzed cavity dimension, low cylinder wall temperatures have an insignificant effect on the cavity emitted energy, as seen on the left of each Fig. 5 plot. As the cylinder temperature increases, thereby moving right in each Fig. 5 plot, cylinder surface temperatures and emissivity values have an increasing effect on the energy emitted from the cavity. The set of figures also include for comparison Sparrow's isothermal theoretical points and the limiting solution. Sparrow's theoretical points are represented at temperature ratios of one, which corresponds to the Fig. 4 isothermal analysis.

The limiting solution in both Fig. 4 and Fig. 5(a) at small L/R ratios is the disk surface emissivity value, Eq. (7). For these extremely shallow nonisothermal cylinder cavities, the cavity wall temperatures have little effect on cavity apparent emissivity values, as indicated by the nearly horizontal lines in Fig. 5(a).

The limiting solution in Fig. 5(b) to (f) is the disk surface view factor value if the cavity surfaces are represented as blackbody surfaces (perfect absorbers of radiation). The view factor values from the numerical ray tracing technique were compared to an independent solution (Kreith, 1965), which resulted in nearly identical values. The limiting solution breaks down for nonblackbody surfaces when the L/R dimension and the surface emissivity value permit energy (rays) to reflect off the cylinder cavity walls and escape out the cavity opening before the energy is totally absorbed.

Linear cylinder wall temperature effects (as illustrated in Fig. 2) are shown for several cavity dimensions with varying surface emissivity values in Figs. 6(a) to (d). The major distinguishing factor from the previous plotted results is that the temperature ratio on the x-axis now represents exit to disk, by the following equation for environmental temperatures at absolute zero:

$$\text{Temperature ratio} = \frac{T_E - T_\infty}{T_D - T_\infty} = \frac{T_E}{T_D} \qquad (12)$$

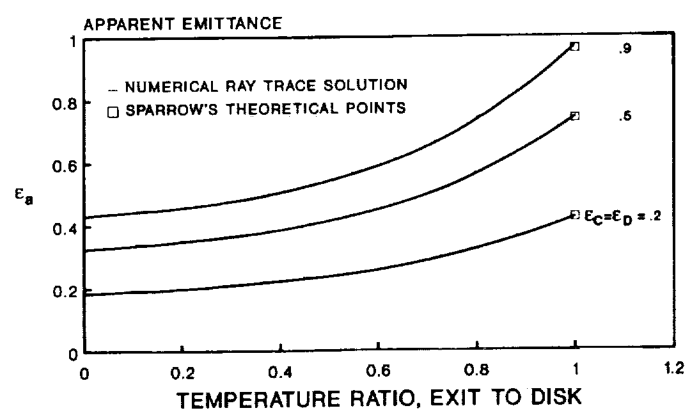


(A) L/R = 1.00.

FIGURE 6. - APPARENT EMITTANCE AS A FUNCTION OF LINEAR WALL TEMPERATURES.

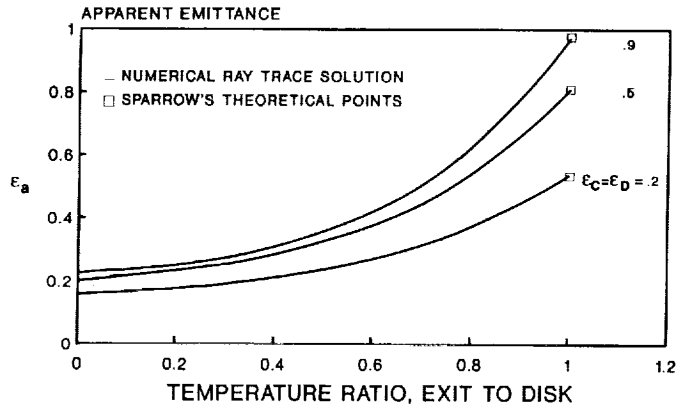


(B) L/R = 2.00.

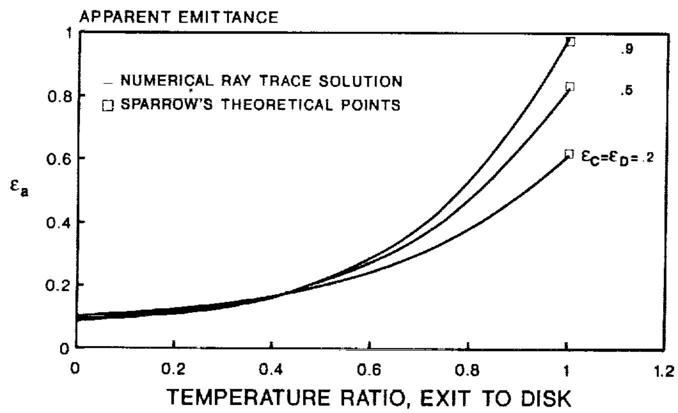


(C) L/R = 4.00.

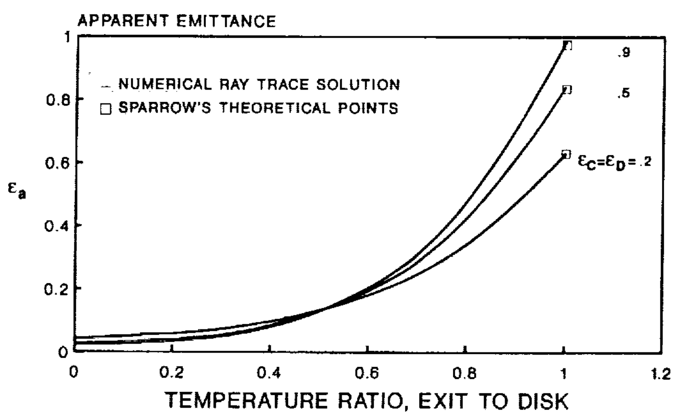


(D) L/R = 8.00.

FIGURE 6. - CONCLUDED.

Inspection of these curves reveals that the same trends occur as in the nonisothermal analysis with uniform wall temperatures (Fig. 5), where the apparent emissivity is dominated by the cylinder wall temperature profiles. In addition, for large cavity L/R values, the plots reveal that upon reaching a specific cylinder wall temperature profile, the relationship between surface emissivity values begins to have a reverse effect on cavity performance. The location where the apparent emissivity curves converge for the various surface emissivity values will be referred to as the cylinder emissivity threshold point or just threshold point. For practical purposes, the locations of these points of convergence are treated as a single point.

As seen by moving from left to right in the apparent emissivity plots of Figs. 6(c) and (d), the effect of surface emissivity values on the energy emitted out the cavity reverses after crossing the temperature threshold location. At the left side of the temperature threshold location, the low exit surface temperatures become a minor source of emitted radiation with higher surface emissivity values causing less emission of disk and cylinder wall energy from the cavity. In contrast, to the right of the temperature threshold location, the higher exit surface temperatures become a major contributing source of emitted radiation where a larger surface emissivity value permits an increase of energy emitted from the duct.

Figs. 7(a) to (d) are also included to display and compare cavity results for nonisothermal uniform and linear cylinder wall temperatures. Note the temperature ratio on the x-axis is displayed above for the linear and below for the uniform temperature curves. Again Sparrow's isothermal theoretical points are displayed in the figures for reference. From this comparison, it can be seen that the higher apparent emissivity values are obtained for the linear wall temperature cases than for the uniform wall temperature cases. This primarily results from the linear analysis containing a higher average cylinder wall temperature than the uniform analysis at any given temperature ratio, thus producing greater emitted energy.

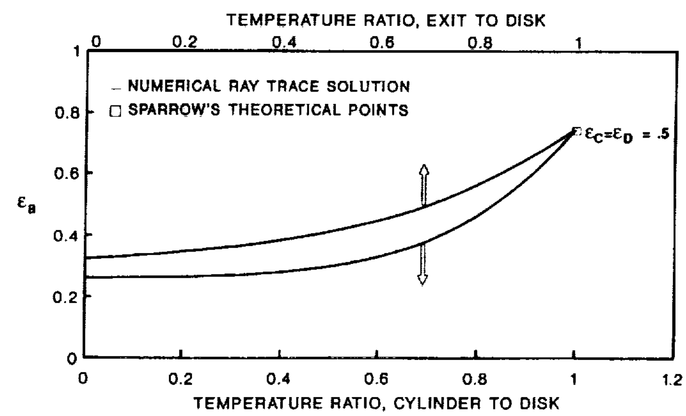


(A) L/R = 1.00.

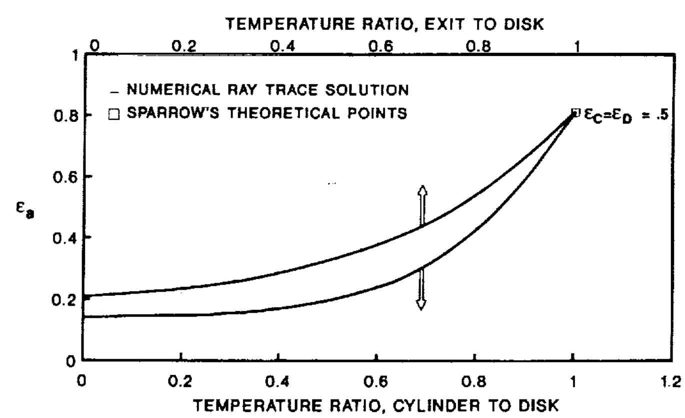


(B) L/R = 2.00.

FIGURE 7. - APPARENT EMITTANCE AS A FUNCTION OF UNIFORM AND LINEAR WALL TEMPERATURES.

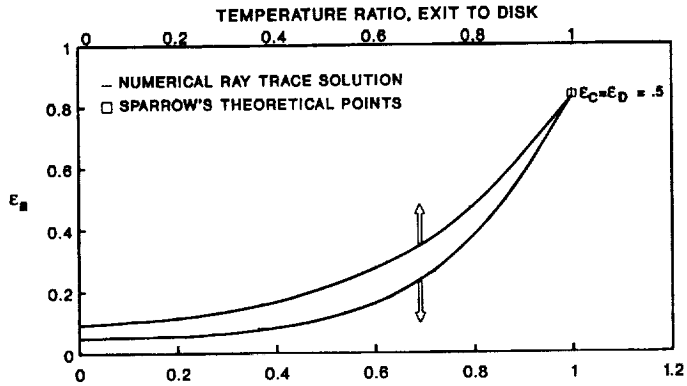


(C) L/R = 4.00.

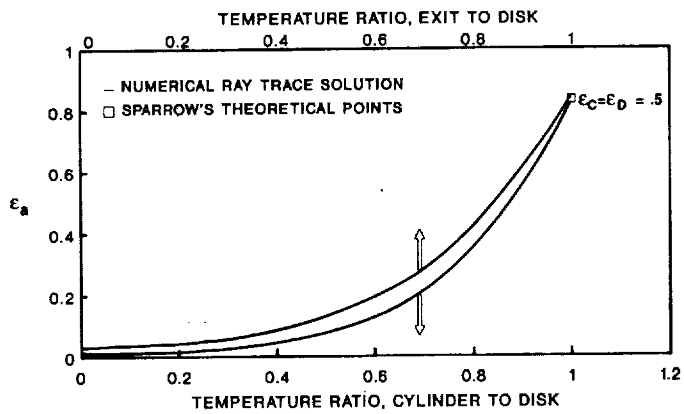


(D) L/R = 8.00.

FIGURE 7. - CONCLUDED.

## CONCLUDING REMARKS

To evaluate simple or complex cavity geometries with variable surface properties, a statistical numerical ray tracing technique used within the computer code NEVADA is an effective tool for obtaining nonuniform energy balance relationships between surfaces. This method can properly evaluate the total radiant energy emitted from complex multisectioned cavities and the radiation exchanged from individual sections within the cavity. The cavities need not be sectioned into individual surfaces with uniform incident radiant energy distributions, but rather surfaces only to define the cavity geometry. For isothermal cylindrical cavities the numerical ray tracing technique compares exactly with other known theoretical solutions and limiting solutions. For relatively small cavities (L/R less than 2) the resistance network (electrical circuit) method accurately predicts the radiation emitted from the cavity for the entire range of surface emissivity values. For larger cavities the resistance network requires sectioning the cavity surfaces into uniform energy distributed sections which may lead to an extremely complicated solution process.

For nonisothermal cylindrical cavities with either uniform or linearly varying cylinder wall temperatures, the energy emitted from the cavity is a function of cavity surface emissivity value and both cavity size and surface temperature except for relatively shallow cavities. For such cavities, with cylinder wall length smaller than cavity radius, emitted energy becomes much less dependent on cylinder surface temperatures and more dependent on disk surface emissivity values. For cavities with linear cylindrical wall temperature profiles, there exist temperature threshold locations which cause a reversal of the surface emissivity effect on the energy emitted out the cavity.

By plotting the theoretical points with the numerical ray tracing results and with limiting solutions, one can accurately grasp the effect of surface temperatures and surface emissivity values on energy emitted from various cavity configurations. This numerical ray tracing technique can enable one to analyze the nonuniform energy distributions within cavities which are separated into various sections with different temperature profiles and different emissivity values.

## REFERENCES

Buckley, H., 1928, "Radiation from Inside a Circular Cylinder," Philosophical Magazine, Vol. 6, pp. 447-457.

Buckley, H., 1927, "Radiation from the Interior of a Reflecting Cylinder," Philosophical Magazine, Vol. 4, pp. 753-762.

Eckert, E., 1935, "Das Strahlungsverhaltnis von Flachen mit Einbuchtungen und von Zylindrischen Bohrungen", Archiv fuer Warmewirtschaft, Vol. 16, No. 5, pp. 135-138.

Holman, J.P., 1986, Heat Transfer, Sixth ed., McGraw-Hill Book Company, New York, NY.

Kreith, F., 1965, Principles of Heat Transfer, Second ed., International Textbook Company, Scranton, PA.

Siegel, R., and Howell, J.R., 1981, Thermal Radiation Heat Transfer, Second ed., Hemisphere Publishing Corporation, Washington, DC.

Sparrow, E.M., and Cess, R.D., 1966, Radiation Heat Transfer, Wadsworth Publishing Company, Belmont, CA.

Sparrow, E.M., Albers, L.U., and Eckert, E.R.G., 1963, "Thermal Radiation Characteristics of Cylinder Enclosures," Journal of Heat Transfer, Vol. 85, No. 1, pp. 73-81.

Sparrow, E.M., Albers, L.U, 1960, "Apparent Emissivity and Heat Transfer in a Long Cylindrical Hole," Journal of Heat Transfer, Vol. 82, No. 3, pp. 253-255.

Turner, R.C., 1988, "NEVADA Software Package User's Manual," Ninth ed., Ver. 14, Turner Associates Consultants.

NASA
National Aeronautics and Space Administration

# Report Documentation Page

| | | |
|---|---|---|
| 1. Report No. NASA TM-102527 | 2. Government Accession No. | 3. Recipient's Catalog No. |
| 4. Title and Subtitle<br>Thermal Radiation Characteristics of Nonisothermal Cylindrical Enclosures Using a Numerical Ray Tracing Technique | | 5. Report Date |
| | | 6. Performing Organization Code |
| 7. Author(s)<br>Joseph F. Baumeister | | 8. Performing Organization Report No.<br>E-5335 |
| | | 10. Work Unit No.<br>505-62 |
| 9. Performing Organization Name and Address<br>National Aeronautics and Space Administration<br>Lewis Research Center<br>Cleveland, Ohio 44135-3191 | | 11. Contract or Grant No. |
| | | 13. Type of Report and Period Covered<br>Technical Memorandum |
| 12. Sponsoring Agency Name and Address<br>National Aeronautics and Space Administration<br>Washington, D.C. 20546-0001 | | 14. Sponsoring Agency Code |

15. Supplementary Notes

Prepared for the 5th Thermophysics and Heat Transfer Conference cosponsored by the AIAA and ASME, Seattle, Washington, June 18-20, 1990.

16. Abstract

Analysis of energy emitted from simple or complex cavity designs can lead to intricate solutions due to nonuniform radiosity and irradiation within a cavity. A numerical ray tracing technique was applied to simulate radiation propagating within and from various cavity designs. To obtain the energy balance relationships between isothermal and nonisothermal cavity surfaces and space, the computer code NEVADA was utilized for its statistical technique applied to numerical ray tracing. The analysis method was validated by comparing results with known theoretical and limiting solutions, and the electrical resistance network method. In general, for nonisothermal cavities the performance (apparent emissivity) is a function of cylinder length-to-diameter ratio, surface emissivity, and cylinder surface temperatures. The extent of nonisothermal conditions in a cylindrical cavity significantly affects the overall cavity performance. Results are presented over a wide range of parametric variables for use as a possible design reference.

| | |
|---|---|
| 17. Key Words (Suggested by Author(s))<br>Cavity radiation propagating<br>Ray tracing<br>NEVADA program | 18. Distribution Statement<br>Unclassified – Unlimited<br>Subject Category 34 |

| 19. Security Classif. (of this report) | 20. Security Classif. (of this page) | 21. No. of pages | 22. Price* |
|---|---|---|---|
| Unclassified | Unclassified | 8 | A02 |

NASA FORM 1626 OCT 86

*For sale by the National Technical Information Service, Springfield, Virginia 22161